Surfactant-Templated Inorganic Lamellar and Non-Lamellar Hybrid Phases Containing Adamantane $[Ge_4Se_{10}]^{4-}$ Anions

Michael Wachhold and Mercouri G. Kanatzidis*

Department of Chemistry and Center for Fundamental Materials Research, Michigan State University, East Lansing, Michigan 48824

Received February 8, 2000. Revised Manuscript Received May 22, 2000

The metathesis reaction of $K_4Ge_4Se_{10}$ with various alkyl tri- and dimethylammonium halides $[C_nH_{2n+1}N(CH_3)_{3-m}H_m]X$ (n = 8, 9, 10, 12, 14, 16, 18; m = 0, 1; X = Cl, Br) led to several new surfactant−inorganic template phases containing selenogermanate adamantane units $[Ge_4Se_{10}]^{4-}$. The crystal structures of phases with shorter alkylammonium chains (n = 8 and 9) have been determined by single-crystal X-ray crystallography; octyltrimethylammonium decaselenotetragermanate, $[n\text{-}C_8H_{17}N(CH_3)_3]_4Ge_4Se_{10}$ (C8−GeSe), monoclinic, space group $C2/c$, $Z = 4$, $a = 34.2324(9)$ Å, $b = 10.9213(3)$ Å, $c = 19.2700(5)$ Å, $\beta = 104.567°$; nonyltrimethylammonium decaselenotetragermanate $[n\text{-}C_9H_{19}N(CH_3)_3]_4Ge_4Se_{10}$ (C9−GeSe), triclinic, space group $P\bar{1}$, $Z = 2$, $a = 10.7799(2)$ Å, $b = 18.1172(3)$ Å, $c = 19.0075(1)$ Å, $\alpha = 91{,}881(1)°$, $\beta = 90.017(1)°$, $\gamma = 98.767(1)°$; octyldimethylammonium decaselenotetragermanate $[n\text{-}C_8H_{17}N(CH_3)_2H]_4Ge_4Se_{10}$ (ODA−GeSe) tetragonal, space group I_1/a, $Z = 4$, $a = 18.6462(1)$ Å, $c = 19.2038(1)$ Å. C8−GeSe and C9−GeSe are composed of parallel layers of $[Ge_4Se_{10}]^{4-}$ anions in a pseudohexagonal arrangement, separated by the charge-balancing surfactant cations. While C9−GeSe contains bilayers of *parallel* interdigitating surfactant hydrocarbon chains, the shorter chains in C8−GeSe show a *crisscross*-like arrangement. The presence of hydrogen bonds in ODA−GeSe leads to the formation of a novel nonlamellar phase with *isolated* adamantane clusters whereby each is surrounded by four surfactant molecules. At the inorganic−organic interface, the Se···H contacts of the surfactant cations to the terminal Se atoms (Se_t) of the adamantane cluster are unusually short (2.38(5) Å), leading to strong N−H···Se hydrogen bonds. $[(n\text{-}C_4H_9)_3NH]_4Ge_4Se_{10}$ has a very similar arrangement of the organic/inorganic building units to that of ODA−GeSe, including the strong N−H···Se hydrogen bonds.

Introduction

MCM-41[1] and related compounds[2] are mesostructured silicates and aluminosilicates with large pore sizes between 20 and 100 Å that hold promise for catalytic, environmental, gas absorption, and other applications.[3] Recently, efforts have been started by us[4,5] and other groups[6] to establish synthetic methodologies for non-oxidic, e.g. thio- or seleno-based, materials. The combination of "mesoporous properties" like catalysis or absorption with typical "semiconductor properties" such as those found in chalcogenide materials promises to open new doors to novel multifunctional materials. We chose the adamantane anion $[Ge_4Q_{10}]^{4-}$ (Q = S, Se) as a suitable analogue to silicate/aluminosilicate materials, since it possesses the desired tetrahedral topology and is furthermore known to be stable in water over a wide pH range.[7] Already, on a mainly aqueous route, we were able to synthesize mesostructured metal germanium sulfide and selenide materials with the well-defined stoichiometry $[surfactant]_2M^{II}Ge_4Q_{10}$ (Q = S, Se), by ion-exchange and electrostatic self-assembly reactions of $[Ge_4Q_{10}]^{4-}$ with various divalent transition metal ions M^{II} (Zn^{2+}, Cd^{2+}, Ni^{2+}, Co^{2+}, Mn^{2+}) and water-soluble surfactant templates $C_nH_{2n+1}NMe_3Br$ (n = 12, 14, 16, 18).[4,5,8] All materials possess a three-dimensional $[MGe_4Q_{10}]^{2-}$ framework which is perforated by wormhole-like channels containing the surfactant molecules, although in the case of Mn^{2+}, hydrothermal synthesis conditions give $(CTA)_2MnGe_4S_{10}$ (CTA = $C_{16}H_{33}NMe_3^+$)

(1) (a) Kresge, C. T.; Leonowicz, M. E.; Roth, W. J.; Vartuli, J. C.; Beck, J. S. *Nature* **1992**, *359*, 710−712. (b) Beck, J. S.; Vartuli, J. C.; Roth, W. J.; Leonowicz, M. E.; Kresge, C. T.; Schmitt, K. D.; Chu, C. T−W., Olson, D. H.; Sheppard, E. W.; McCullen, S. B.; Higgins, J. B.; Schlenker, J. L. *J. Am. Chem. Soc.* **1992**, *114*, 10834.

(2) (a) Zhao, D.; Luan, Z.; Kevan, L. *Chem. Commun.* **1997**, 1009. (b) Holland, B. T.; Isbester, P. K.; Blanford, C. F.; Munson, E. J. Stein, A. *J. Am. Chem. Soc.* **1997**, *116*, 6796. (c) Cheng, S.; Tzeng, J.-N.; Hsu, B.-Y. *Chem. Mater.* **1997**, *9*, 1788. (d) Kimura, T.; Sugahara, Y.; Kuroda, K. *Chem. Commun.* **1998**, 559.

(3) (a) Ying, J. Y.; Mehnert, C. P.; Wong, M. S. *Angew. Chem., Int. Ed. Engl.* **1999**, *38*, 56. (b) Sayari, A. *Chem. Mater.* **1996**, *8*, 1840.

(4) Wachhold, M.; Rangan, K. K.; Billinge, S. J. L.; Petkov, V.; Heising, J.; Kanatzidis, M. G. *Adv. Mater.* **2000**, *12*, 85.

(5) Wachhold, M.; Rangan, K. K.; Billinge, S. J. L.; Petkov, V.; Heising, J.; Kanatzidis, M. G. *J. Solid State Chem* **2000**, in press.

(6) See e.g.: (a) Jiang, T.; Ozin, G. A. *J. Mater. Chem.* **1998**, *8*, 1099−1108. (b) Jiang, T.; Ozin, G. A.; Bedard, R. L. *J. Mater. Chem.* **1998**, *8*, 1641−1648. (c) Fröba, M.; Oberender, N. *J. Chem. Soc. Chem. Commun.* **1997**, 1729−1730. (d) Li, J. Q.; Kessler, H.; Delmotte, L. *J. Chem. Soc., Faraday Trans.* **1997**, *93*, 665−668. (e) Li, J. Q.; Delmotte, L.; Kessler, H. *J. Chem. Soc., Chem. Commun.* **1996**, 1023−1024.

(7) Krebs, B. *Angew. Chem., Int. Ed. Engl.* **1983**, *22*, 113.

(8) Rangan, K. K.; Billinge, S. J. L.; Petkov, V.; Heising, J.; Kanatzidis, M. G. *Chem. Mater.* **1999**, *11*, 2629.

10.1021/cm000102o CCC: $19.00
Published on Web 09/06/2000

with *hexagonally ordered* pores. Similarly, Ozin and co-workers synthesized framework materials of the general type $(CTA)_2M^{II}_2Ge_4S_{10}$ (M^{II}= Zn^{2+}, Ni^{2+}, Cu^{+}, and Co^{2+}) with a *nonaqueous route* (with formamide) which also possess hexagonally ordered pores.[9]

A crucial process for the synthesis of these materials is the liquid-crystal template approach, and a number of different electrostatic and dipolar interaction possibilities have been discussed as intermediates during product formation in many reaction systems (i.e., S^+I^-, S^0 I^0, $S^+X^-I^+$, $S^-M^+I^-$, etc).[3a] In the case of lamellar phases, for example, the arrangement of *n*-alkyltrimethylammonium and related surfactants in bilayers has been studied by electron microscopy[10] or differential thermal analysis (DTA)[11] and the similarity of the assembly to those of phospholipids, found in biological membranes, has been shown. Therefore, accurately determined crystal structures of surfactant-templated materials[12] containing arrays of inorganic species have received much attention, to gain better understanding of surfactant behavior. Ultimately, this information should help us use these surfactant templates more efficiently. Furthermore, structural information on surfactant-based phases and a precise understanding of surfactant−anion interactions in the solid-state could be used to construct more accurate models for representing self-assembled monolayers and lipid bilayers. In addition, such lamellar phases can serve as suitable precursors for the construction of micro- and mesoporous phases. We have already studied adamantane cluster $[Ge_4S_{10}]^{4-}$ salts with various surfactants[13] and reported on the single-crystal structures of the lamellar $(R-NMe_3)_4Ge_4S_{10}$ compounds (R = *n*-$C_{12}H_{25}$, *n*-$C_{14}H_{29}$, *n*-$C_{16}H_{33}$, and *n*-$C_{18}H_{37}$) and their physicochemical behavior under a variety of conditions.

In general, well-characterized lamellar sulfide phases with surfactant species are rare. For example, Li and co-workers have reported the structure and some properties of the water-containing, lamellar tin sulfide $[n\text{-}C_{12}H_{25}NH_3]_4Sn_2S_6{\cdot}2H_2O$;[14] in a somewhat older paper, Dehnicke et al. described the crystal structure of $[C_{14}H_{29}NMe_3]_2S_6$ which contains S_6^{2-} chains.[15]

To get better insight into the organization of long chain surfactant molecules in the presence of chalcogenido anions, we explored the synthesis of new surfactant-containing mesostructured phases containing the *seleno* adamantane anion $[Ge_4Se_{10}]^{4-}$. We were especially interested in their structural evolution under the variation of (a) the surfactant alkyl chain length *n*, (b) the strength of interaction at the organic−inorganic interface, and (c) the surfactant shape. We varied (b) and (c) by using cationic surfactant molecules $[C_nH_{2n+1}NMe_{3-m}H_m]^+$ with $m = 0$ or 1. Much stronger organic−inorganic interactions can be expected for $m = 1$, because of additional hydrogen bridges possible at the organic−inorganic interface (i.e., N−H···Se). All lamellar phases of the series $[(C_nH_{2n+1})N(CH_3)_3]_4Ge_4Se_{10}$ (hereafter referred to as C*n*−GeSe) with $n = 8$, 9, 10, 12, 14, 16, 18 have been synthesized and characterized by powder diffraction. Additionally, single-crystal structure analyses of the first members C8−GeSe and C9−GeSe of this series have been performed. The arrangement and conformation of the surfactant molecules with different chain lengths are discussed. By introducing surfactant molecules with N−H groups, the structure assembly process changes dramatically and stabilizes the nonlamellar compound $[n\text{-}C_8H_{17}N(CH_3)_2H]_4Ge_4Se_{10}$ (ODA−GeSe). This compound adopts tetragonal symmetry and contains *single units* "$[n\text{-}C_8H_{17}N(CH_3)_2H]_4Ge_4Se_{10}$", assembling a framework held together by van der Waals interactions.

Experimental Section

Syntheses. *K_2Se.* K_2Se was prepared by reacting stoichiometric amounts of the elements in liquid ammonia.

$K_4Ge_4Se_{10}$. $K_4Ge_4Se_{10}$ was prepared by heating stoichiometric amounts of thoroughly mixed K_2Se, Ge, and Se (1:2:4) in evacuated quartz ampules at 850 °C for 32 h. This procedure gave an air sensitive, shiny yellow powder, which was stored in a nitrogen-filled glovebox.

Octyldimethylammonium chloride ($n\text{-}C_8H_{17}N(CH_3)_2H)Cl$. Octyldimethylamine ($C_8H_{17}N(CH_3)_2$) was dissolved in a 1:1 solution (by volume) of acetone and H_2O. Under slight heating (∼50 °C) a stoichiometric amount (1:1) of 0.1 M HCl was added slowly upon stirring, which led immediately to a white precipitate. The mixture is heated for another hour to evaporate most of the mother liquor. The obtained powder of octyldimethylammonium chloride is dried in a vacuum for several hours, over a water bath at about 50 °C (yield > 80%).

C8−GeSe, $[n\text{-}C_8H_{17}N(CH_3)_3]_4Ge_4Se_{10}$. A 4:1 ratio of $C_8H_{17}N(CH_3)_3Br$ and $K_4Ge_4Se_{10}$ was dissolved in a 1:1 acetone/H_2O solution (by volume) at room temperature. Several days later large yellow crystals of C8−GeSe (up to several mm) could be isolated from the solution (yield typically >90%). They were dried in a vacuum and kept in the glovebox, since the compound is very unstable against oxidation and turns first red and then black upon exposure to air within a few hours. EDS analysis confirms a 2:5 ratio of Ge and Se. The same compound could also be obtained from a 1:1 solution (by volume) of methanol and H_2O, but the crystal quality was not as good, and the crystals were considerably smaller.

C9−GeSe, $[(n\text{-}C_9H_{19}N(CH_3)_3]_4Ge_4Se_{10}$. Similar to OTA−GeSe, NTA−GeSe was synthesized by dissolving a 4:1 ratio of $C_9H_{19}N(CH_3)_3Br$ and $K_4Ge_4Se_{10}$ in a 1:1 acetone/H_2O solution. In this case, the solution was heated slightly to ∼45 °C to ensure complete dissolution of the reactants. Yellow crystals (yield >80%) of C9−GeSe were collected and dried in a vacuum (EDS Ge:Se 1:2.5).

ODA−GeSe, $[n\text{-}C_8H_{17}N(CH_3)_2H]_4Ge_4Se_{10}$. Four equivalents of $[(n\text{-}C_8H_{17}N(CH_3)_2H)Cl]$ were dissolved in a 1:1 ratio of acetone:H_2O, together with 1 equiv of $K_4Ge_4Se_{10}$. The reactants dissolve completely after slight heating (∼40 °C). One day later, large yellow needles (up to ∼3 mm) of ODA−GeSe could be isolated from the mother liquor. The compound is air stable for several hours, but turns red after several days (EDS Ge:Se 1:2.5).

$[n\text{-}C_nH_{2n+1}N(CH_3)_3]_4Ge_4Se_{10}$ salts with $n = 10$, 12, 14, 16, 18 (Cn−GeSe). These compounds were synthesized by metath-

(9) (a) MacLachlan, M.; Coombs, N.; Ozin, G. A. *Nature* **1999**, *397*, 681−684. (b) MacLachlan, M. J.; Coombs, N.; Bedard, R. L.; White, S.; Thompson, L. K.; Ozin, G. A. *J. Am. Chem. Soc.* **1999**, *121*, 12005.

(10) (a) Kunitake, T.; Okahata, Y.; Tamaki, K.; Kumamaru, F.; Takayanagi, M. *Chem. Lett.* **1977**, 367. (b) Kunitake, T.; Okahata, Y. *J. Am. Chem. Soc.* **1977**, *99*, 3860.

(11) Kajiyama, T.; Kumano, A.; Takayanagi, M.; Okahata, Y.; Kunitake, T. *Contemporary Topics in Polymer Science*; Bailey, W. J., Tsuruta, T., Eds.; Vol. 4, p 829, Plenum Press: New York, 1984.

(12) Janauer, G. G.; Dobley, A.; Zavalij, P.; Whittingham, M. S. *Chem. Mater.* **1997**, *9*, 647. Oliver, S. R. J.; Lough, A. J., Ozin, G. A. *Inorg. Chem.* **1998**, *37*, 5021. Ayyappan, S.; Ulagappan, N.; Rao, C. N. R. *J. Mater. Chem.* **1996**, *6*, 1737. Fosse, N.; Caldes, M.; Joubert, O.; Ganna, M.; Brohan, L. *J. Solid State Chem.* **1998**, *139*, 310. (c) Fosse, N.; Brohan, L. *J. Solid State Chem.* **1999**, *145*, 655.

(13) Bonhomme, F.; Kanatzidis, M. G. *Chem. Mater.* **1998**, *10*, 1153−1159.

(14) Li, J.; Marler, B.; Kessler, H.; Soulard, M.; Kallus, S. *Inorg. Chem.* **1997**, *36*, 4697.

(15) Weller, F.; Adel, J.; Dehnicke, K. *Z. Anorg. Allg. Chem.* **1987**, *548*, 125.

esis reactions of (n-$C_nH_{2n+1}N(CH_3)_3$)Br and $K_4Ge_4Se_{10}$ in acetone−H_2O or MeOH−H_2O mixtures. Since with longer alkyl chain length of the surfactant molecule it is necessary to use higher reaction temperatures, the synthesis procedures vary slightly (depending on n) to ensure complete dissolution of the reactants. [n-$C_{10}H_{21}N(CH_3)_3$]$_4Ge_4Se_{10}$ and [n-$C_{12}H_{25}N(CH_3)_3$]$_4$-Ge_4Se_{10} are obtained by heating the solvent mixture to the boiling point (∼80 °C) and slowly cooling until incipient crystallization. On the other hand, C14/C16/C18−GeSe were obtained by sealing the reactants in thick-walled Pyrex tubes and heating the mixtures to ∼100−120 °C, with subsequent cooling to room temperature over several days.

[(n-C_4H_9)$_3$NH]$_4Ge_4Se_{10}$. This compound was first observed as a decomposition product of the solventothermal reaction of (n-$C_{16}H_{33}$)N(n-C_4H_9)$_3$Br and $K_4Ge_4Se_{10}$ in H_2O−acetone at 120 °C. To synthesize the product on a direct path, we set up a 4:1 reaction of (n-C_4H_9)$_3$N and $K_4Ge_4Se_{10}$ in a H_2O−acetone mixture. The solution was slightly heated to 40−50 °C and 4 equiv of protons was added in the form of a 0.1 M HCl aqueous solution. The solution was cooled slowly to room temperature and allowed to stand (N_2 atmosphere) in an open container for several days. Upon slow solvent evaporation, large orange-yellow prisms were formed, with dimensions up to 1.5 mm. The crystals were isolated and dried with ether (yield > 80%).

Physical Measurements. *Powder X-ray Diffraction.* Analyses were performed using a computer-controlled INEL CPS120 powder diffractometer in asymmetric reflection mode, operating at 40 kV/20 mA, with graphite-monochromatized Cu Kα radiation. The diffractometer was calibrated in the low-angle region using hexadecyltrimethylammonium bromide (C_{16}Br) as external standard.

Raman and Infrared Spectroscopy. Raman spectra of suitable single crystals with a clean surface were recorded on a Holoprobe Raman spectrograph equipped with a 633 nm helium−neon laser and a CCD camera detector. The instrument was coupled to an Olympus BX60 microscope. The spot size of the laser beam was 10 mm when a 50× objective lens was used. Infrared spectra, in the IR region (6000−400 cm^{-1}) or far-IR region (600−100 cm^{-1}), were recorded on a computer-controlled Nicolet 750 Magna-IR Series II spectrometer equipped with a TGS/PE detector and a silicon beam splitter in 2 cm^{-1} resolution. The samples were mixed with ground, dry CsI and pressed into translucent pellets.

Solid State UV/Vis/Near-IR Spectroscopy. UV−vis−near-IR diffuse reflectance spectra were obtained at room temperature on a Shimadzu UV-3101PC double-beam, double-monochromator spectrophotometer in the wavelength range of 200−2500 nm. The instrument is equipped with an integrating sphere and controlled by a PC. $BaSO_4$ powder was used as a reference (100% reflectance) and base material, on which the ground powder sample was coated. Reflectance data were converted to absorbance data as described elsewhere.[16] The band gap energy value was determined by extrapolation from the linear portion of the absorption edge in a (a/S) versus E plot.

Thermogravimetric Analyses (TGA). TGA data were obtained with a computer-controlled Shimadzu TGA-50 thermal analyzer. Typically 25−30 mg of sample was placed in a quartz bucket and heated in a nitrogen flow of 50 mL/min with a rate between 2 and 10 °C/min. The residues from the TGA experiments were examined by X-ray powder diffraction.

Differential Scanning Calorimetry (DSC). DSC experiments were performed on a computer-controlled Shimadzu DSC-50 thermal analyzer. About 10−15 mg of samples was sealed under nitrogen in an aluminum container. An empty container was used as a reference. All measurements were done with a heating rate of 2 °C/min.

Semiquantitative Microprobe Analyses (EDS). The analyses were performed using a JEOL JSM-35C scanning electron microscope (SEM) equipped with a Tracor Northern energy dispersive spectroscopy (EDS) detector. Data acquisition was performed several times in different areas of the samples using an accelerating voltage of 20 kV and 45 s accumulation time.

X-ray Crystallography. Single crystals of all crystalline compounds (crystal dimensions: ODA−GeSe, 0.30 × 0.30 × 0.22 mm; C8−GeSe, 0.31 × 0.22 × 0.03 mm, C9−GeSe, 0.40 × 0.30 × 0.02 mm; [n-Bu_3NH]$_4Ge_4Se_{10}$, 0.31 × 0.15 × 0.13 mm) were sealed in glass capillaries (diameter 0.5 or 0.7 mm, wall thickness $^1/_{100}$ mm) and mounted on a goniometer head. Crystallographic data sets for the compounds were collected on a Siemens Platform CCD diffractometer using graphite-monochromatized Mo Kα radiation. The data were collected over a full sphere of reciprocal space, up to 58° in 2θ. The individual frames were measured with an θ rotation of 0.3° and acquisition times of 15−30 s. The SMART[17] software was used for the data acquisition and SAINT[18] for the data extraction and reduction. The absorption correction was performed using SADABS.[19]

Structure solutions and refinements were performed with the SHELXTL package of crystallographic programs.[20] Intensity statistics indicated unambiguously that all compounds crystallize in centrosymmetric space groups. The structure of ODA−GeSe was solved in the tetragonal space group $I4_1/a$, C8−GeSe and [n-Bu_3NH]$_4Ge_4Se_{10}$ in the monoclinic space group $C2/c$, and C9−GeSe in the triclinic space group $P\bar{1}$. The structures were solved by direct methods, which gave the positions of the adamantane clusters (Ge and Se atoms). In consecutive least-squares refinements, all carbon and nitrogen atoms were gradually found from subsequent difference Fourier syntheses. All non-hydrogen atoms of ODA−GeSe, C8−GeSe, and [n-Bu_3NH]$_4Ge_4Se_{10}$ were refined anisotropically. All non-hydrogen atoms of C9−GeSe with the exception of nine carbon atoms (nonpositive defined if anisotropic) were refined anisotropically. Additionally, the N-bonded hydrogen atom of ODA−GeSe was also found in the Fourier map and refined without constraints. All other hydrogen atoms in all four structures were placed geometrically and refined with a riding model. Complete data collection parameters and details of the structure solution and refinement for the compounds are given in Table 1.

Results and Discussion

Synthesis. The metathesis reactions of ($C_nH_{2n+1}N(CH_3)_{3-m}H_m$)X ($n$ = 8, 9, 10, 12, 14, 16, 18; m = 0, 1; X = Cl, Br) and $K_4Ge_4Se_{10}$ led to several new surfactant-containing selenogermanates. Upon mixing of the alkyldi- or -trimethylammonium salt and $K_4Ge_4Se_{10}$ in the appropriate solvent mixtures, the products form readily, according to eq 1:

$$4[C_nH_{2n+1}N(CH_3)_{3-n}H_n]X + K_4Ge_4Se_{10} \rightarrow [C_nH_{2n+1}N(CH_3)_{3-n}H_n]_4Ge_4Se_{10} + 4KX \quad (n = 0, 1;\ X = Cl, Br)$$

Single crystals of ODA−GeSe and C8−GeSe formed at room temperature after a short period of time (usually 1 day) from a solution of approximately 1:1 volume of acetone and H_2O. The solvent ratio turned out to be noncritical, since other similar ratios also lead to the formation of large crystals after one or more days, as long as all reactants are completely dissolved. Additionally, we could observe the formation of the same products from mixtures of methanol and H_2O, although

(16) McCarthy, T. J.; Ngeyi, S.-P.; Liao, J.-H.; DeGroot, D. C.; Hogan, T.; Kannewurf, C. R.; Kanatzidis, M. G. *Chem. Mater.* **1993**, *5*, 331.

(17) SMART, Version 5; Siemens Analytical X-ray Systems, Inc., Madison, WI, 1998.

(18) SAINT, Version 4; Siemens Analytical X-ray Systems, Inc., Madison, WI, 1994−1996.

(19) SADABS: Sheldrick, G. M., University of Göttingen, Germany.

(20) Sheldrick, G. M.; SHELXTL, Version 5.1, Siemens Analytical X-ray Systems, Inc., Madison, WI, 1997.

Table 1. Crystal Data and Structure Refinement for C8−GeSe, C9−GeSe, ODA−GeSe, and $[n\text{-}Bu_3NH]_4Ge_4Se_{10}$

	C8−GeSe	C9−GeSe	ODA−GeSe	$[n\text{-}Bu_3NH]_4Ge_4Se_{10}$
empirical formula	$C_{44}H_{104}N_4Ge_4Se_{10}$	$C_{48}H_{112}N_4Ge_4Se_{10}$	$C_{40}H_{96}N_4Ge_4Se_{10}$	$C_{48}H_{108}N_4Ge_4Se_{10}$
formula weight	1769.27	1825.38	418.74	910.67
temp (K)	153	153	153	295
crystal system	monoclinic	triclinic	tetragonal	monoclinic
space group	*C*2/*c* (#15)	P-1	$I4_1/a$	*C*2/*c*
a (Å)	34.2324(9)	10.7799(2)	18.6462(1)	26.439(3)
b (Å)	10.9213(3)	18.1172(3)	18.6462(1)	18.889(2)
c (Å)	19.2700(5)	19.0075(1)	19.2038(1)	19.677(2)
α (deg)	90	91.881(1)	90	90
β (deg)	104.567(1)	90.017(1)	90	129.50(1)
γ (deg)	90	98.767(1)	90	90
V (Å^3)	6972.7(3)	3666.79(9)	6676.79(6)	7582.6(15)
Z	4	2	4	4
crystal size (mm)	0.31 × 0.22 × 0.03	0.40 × 0.30 × 0.02	0.30 × 0.30 × 0.22	0.31 × 0.15 × 0.13
crystal shape, color	plate, yellow	plate, yellow	needle, yellow	prism, yellow
no. reflections $F_o > 4\sigma(F_o)$	3461	5551	3189	3306
goodness-of-fit on F^2	0.970	1.016	1.186	0.869
final *R* indices [$I > 2\sigma(I)$]	$R_1 = 0.0705$, $wR_2 = 0.1093$	$R_1 = 0.0780$, $wR_2 = 0.1390$	$R_1 = 0.0366$, $wR_2 = 0.0738$	$R_1 = 0.0603$, $wR_2 = 0.1254$
R indices (all data)	$R_1 = 0.2010$, $wR_2 = 0.1382$	$R_1 = 0.2395$, $wR_2 = 0.1653$	$R_1 = 0.0567$, $wR_2 = 0.0794$	$R_1 = 0.1875$, $wR_2 = 0.1580$
largest diff. peak/hole (e Å^{-3})	0.976 and −0.630	1.738 and −2.278	0.507 and −1.101	0.890 and −0.402

the crystal quality tended to be inferior. To ensure complete dissolution of the nonyltrimethylammonium salt in the formation of C9−GeSe, the 1:1 acetone−H_2O solution is slightly heated to about 40−50 °C. After a few days well-shaped crystals of the product are obtained. Generally, C*n*−GeSe phases with longer alkyl chains (higher *n*) require higher reaction temperatures to form. This was also observed in the corresponding sulfur phases C*n*−GeS with $n = 12, 14, 16, 18$.[13] On the basis of this trend we could synthesize C10−GeSe and C12−GeSe by solution methods (acetone−H_2O or MeOH−H_2O mixtures) at temperatures around 70−80 °C. In comparison, C14−GeSe, C16−GeSe, and C18−GeSe could not be obtained by this method but by *solvothermal crystallization* in closed Pyrex tubes at around 100−120 °C.

X-ray Diffraction Pattern of Lamellar C*n*−GeSe and Non-Lamellar ODA−GeSe. The X-ray powder diffraction patterns of all characterized C*n*−GeSe phases clearly reveal their lamellar character. A characteristic of a lamellar phase is that the diffraction peaks associated with the inorganic layer-to-layer distance (called d_{00l}) are strongly pronounced in comparison to all other peaks (d_{hkl}), which leads to an equidistant peak pattern. Figure 1A−C shows typical XRD patterns for lamellar C*n*−GeSe phases with $n = 8$, 9, and 14. Whereas the phases with shorter surfactant chains ($n = 8$, 9) still show additional peaks besides the strong lamellar (00l) peaks, the higher homologues with $n \geq 10$ show exclusively the d_{001} peaks. The alkyl chain length of a given surfactant C*n* is hereby proportional to the layer-to-layer distance in the crystal structure, as is shown is Figure 2. Therefore, the distance between the inorganic layers can be easily tuned by changing the alkyl substituents of the surfactant molecule. The lamellar basal peaks are very strong due to the preferential orientation of the plate-like crystals of these compounds on the glass slides used for recording the powder patterns. The behavior of a tunable lamellar phase observed here is rather different from what was found in many oxide systems. In silica chemistry, for example, it is well-known that they can occur with hexagonal, cubic, or lamellar structures, depending on reaction

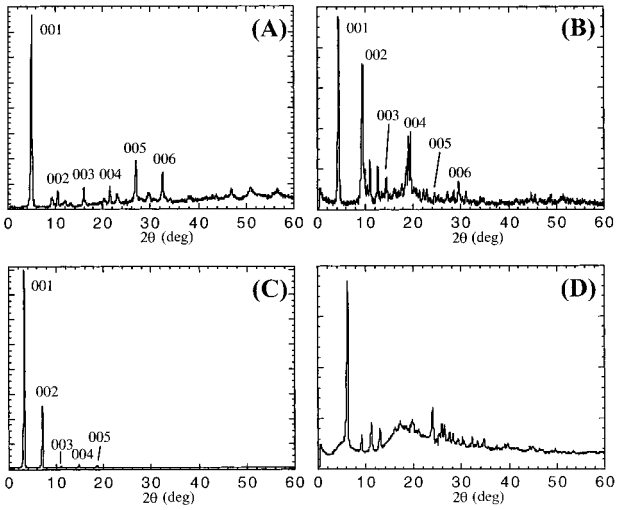

Figure 1. X-ray diffraction patterns of lamellar (A) C8−GeSe, (B) C9−GeSe, (C) C14−GeSe, and nonlamellar (D) ODA−GeSe.

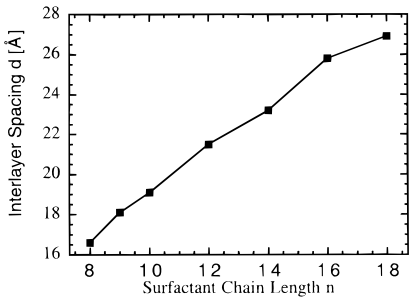

Figure 2. Inorganic layer-to-layer distance (Å) vs alkyl chain length *n* of the surfactant molecule C*n* ($n = 8$, 9, 10, 12, 14, 16, 18) in C*n*−GeSe phases.

conditions and surfactants, however, most work has in fact been done on hexagonal phases.[21] Their structure types go along with the formation of a polymeric framework by condensation reactions of the used (metal) oxide building units.[22] Nevertheless, if in lamellar structure types identical isolated anions are involved,

(21) Beck, J. S.; Vartuli, J. C. *Curr. Opin. Solid State Mater. Sci.* **1996**, *1*, 76.

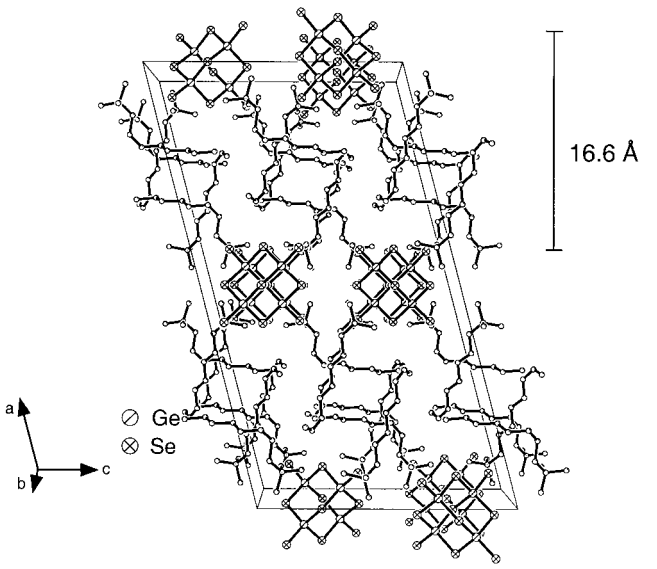

Figure 3. Unit cell of C8−GeSe from [010] direction (H atoms omitted). The $[Ge_4Se_{10}]^{4-}$ layers are separated by the crisscross-like arranged surfactant molecules, with an interlayer distance of 16.6 Å. Selected bond lengths (Å): Ge−Se_t, 2.2541(12)−2.2555(11); Ge−Se_b, 2.3732(12)−2.3818(11); N−C, 1.473(10)−1.521(9); C−C, 1.426(18)−1.550(13); C147−C148, 1.27(2).

a similar trend like the one reported here is observed, as for example in some oxometalates[23] or phosphates.[24]

In contrast to C*n*−GeSe, Figure 1D shows that the X-ray diffraction pattern of ODA−GeSe gives no hint for the presence of a lamellar phase, which at first came as a surprise. This was later understood in terms of its crystal structure. This novel compound and other C*n*−GeSe ($n = 8, 9$) materials will be described in the next section.

Structures. *C8−GeSe.* OTA-GeSe is composed of alternating layers of $[Ge_4Se_{10}]^{4-}$ adamantane clusters and octyltrimethylammonium surfactant molecules (Figure 3). The unlinked adamantane units are very regular, with almost perfect (109.47°) tetrahedral angles at all Ge atoms (107.36−111.78°). They lie on a 2-fold axis, with the bridging selenium atoms Se3 and Se4 serving as the axis pivots. The bridging Ge−Se_b bond lengths are 2.3737(11)−2.3822(10) Å, which is significantly longer than the terminal ones (Ge−Se_t 2.2525(10), 2.2553(10) Å). Within the inorganic layer, the $[Ge_4Se_{10}]^{4-}$ clusters form an array of approximate hexagonal packing (pseudohexagonal arrangement, see ref 13), with each cluster being surrounded by six neighbors. The closest nonbonding Se···Se distance between two clusters is 5.47 Å.

The inorganic adamantane layers are separated from each other by bilayers of noninterdigitating surfactant chains. The trimethylammonium headgroups of the two crystallographic different molecules are hereby positioned toward the adamantane clusters. As can be seen in Figure 3, one of the *n*-C_8H_{17} chains is *perpendicular* to the adamantane layers, whereas the other one is *bent* in the middle and becomes almost parallel to the layers. This is a new arrangement, so far not found in the crystal structures of Cn−GeQ phases (Q = S, Se, see ref 13 and this paper) with longer alkyl chains ($n \geq 9$). This behavior leads to a crisscross-like arrangement of the surfactant molecules; see Figure 3. At the organic−inorganic interface, both headgroups show a number of long C−H···Se contacts (>2.85 Å). This is only slightly shorter than the sum of the van der Waals radii of H and Se (3.0 Å)[25] and is much longer than typical H···Se hydrogen bridges (~2.5 Å).[26] The two surfactant molecules (named C8-I and C8-II) differ significantly in their conformations, as can be seen from Figure 4A. In C8-I it can be seen that N1, the methyl carbon atom C13, and all but the last carbon of the alkyl chain (C141−C147) lie approximately within a plane. The chain shows a *all-eclipsed* conformation, with a trans position of all these atoms (torsion angles 173.97(1.78)−177.63(2.29)°; see Figures 3, 4A). An exception is the chain *end*, which reveals an unusual *eclipsed* conformation of the last four carbon atoms. Hereby, the torsion angle of C145−C146−C147−C148 is only 30.41(5.19)°. As a consequence, the chain of C8-I might suffer from geometrical repulsion which could be a reason for the high out-of-plane temperature factors of these atoms, especially C147. In the second surfactant, C8-II, the chain also possesses an *all-eclipsed* conformation, but it is bent at C243 (Figure 4A). All torsion angles lie around 180°, except the ones with C243 involved as a middle position atom which lie around 60° (C241−C242−C243−C244 = 61.87(1.37)°; C242−C243−C244−C245 = 65.04(1.53)°). As a result, the atoms C23, N2, C241, C242, and C243 lie within one plane and the chain atoms C243−C248 within another, with the two plains arranged almost perpendicular to each other (Figure 4A).

C9−GeSe. C9−GeSe crystallizes in the lower symmetry triclinic space group $P\bar{1}$, but its structural build-up (Figure 5) is closely related to that of C8−GeSe (Figure 3). The compound possesses a lamellar structure, and the $[Ge_4Se_{10}]^{4-}$ adamantane layers have a very similar hexagonal pattern previously described in the last section. There are no significant cluster−cluster interactions (all Se···Se > 5.32 Å), leaving them almost undistorted (see Figure 5). The interdigitating nonyltrimethylammonium molecules separate the adamantane layers from each other by 18.1 Å (Figure 5). Since again no strong hydrogen bonds can form, all C−H··· Se contacts at the organic−inorganic interface are quite long (>2.81 Å). Because of the lower symmetry of the unit cell of C9−GeSe compared to C8−GeSe, we now have four instead of two crystallographically distinguishable surfactants (see Figure 4B; hereafter named C9-I−C9-IV). Hereby, the two surfactant alkyl chains of C9-III and C9-IV are (almost) fully *extended* while the other two (C9-I and C9-II) are *bent* in the middle of the chain. C9-III (Figure 4B(i)) and C9-IV (Figure 4B-(ii)) possess torsion angles close to 180° (C9-III 175.01-(1.11)−179.98(1.32)°; C9-IV: 174.21(1.28)−178.73(1.57)°). An exception is the *tail* of the alkyl chains, where the

(22) Janauer, G. G.; Dobley, A.; Guo, J.; Zavalij, P.; Whittingham, M. S. *Chem. Mater.* **1996**, *8*, 2096. Janauer, G. G.; Dobley, A.; Zavalij, P. Y.; Whittingham, M. S. *Chem. Mater.* **1997**, *9*, 647.

(23) Fosse, N.; Caldes, M.; Joubert, O.; Ganne, M.; Brohan *J. Solid State Chem.* **1998**, *139*, 310.

(24) Oliver, S. R. J.; Lough, A. J.; Ozin, G. A. *Inorg. Chem.* **1998**, *37*, 5021.

(25) (a) Baur, W. H. *Acta Crystallogr.* **1972**, *B28*, 1456. (b) Bondi, A. *J. Phys. Chem.* **1964**, *68*, 441.

(26) Krebs, B.; Hürter, H.-U.; Enax, J.; Fröhlich, R. *Z. Anorg. Allg. Chem.* **1990**, *581*, 141.

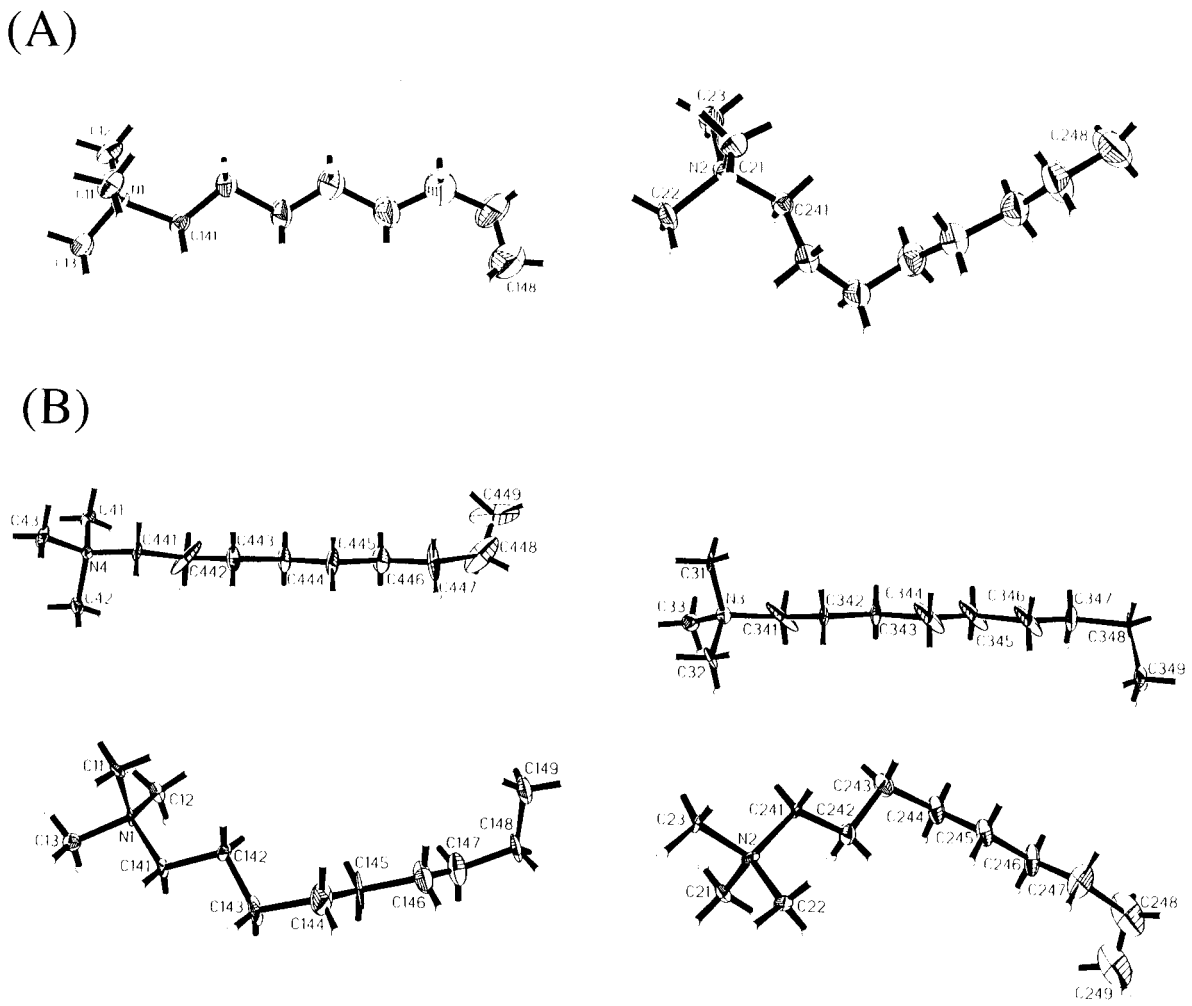

Figure 4. The conformations of the crystallographically independent surfactant molecules (A) C8-I and C8-II in C8−GeSe and (B) C9-I, C9-II, C9-III, and C9-IV in C9−GeSe (the C and N atoms of each chain are labeled).

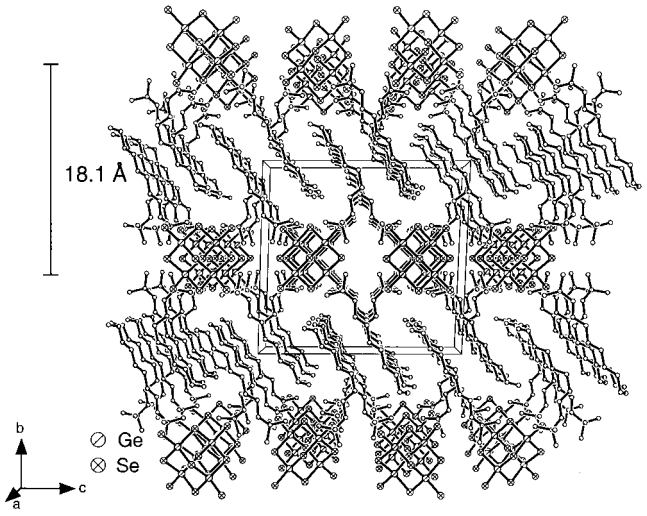

Figure 5. Unit cell of C9−GeSe from the (100)-direction (H-atoms omitted). The inorganic interlayer distance is 18.1 Å. The ammonium headgroups of neighboring surfactant molecules point to opposite adamantane layers and possess antiparallel alkyl chains. Selected bond lengths (Å): Ge−Se_t, 2.255(3)−2.267(2); Ge−Se_b, 2.371(2)−2.387(3); C−N, 1.462(14)−1.594(16); C−C, 1.42(2)−1.61(2).

involved torsion angles are 68.17(2.03)° and 78.46(3.63)°, respectively, corresponding to a gauche conformation of the involved carbon atoms (C346−C349 and C446−C449 for C9-III and C9-IV). The bent surfactant molecules C9-I (Figure 4B(iii)) and C9-II (Figure 4B(iv)) are shorter in their extension, the chains having gauche conformation torsion angles of 77.22(2.06) and 72.68(1.81)° between C142 and C145 (C9-I)/C242 and C245 (C9-II) and 68.71(2.94)/74.14(3.21)° in the tails of the chain (C246−C249 and C346−C349). In contrast to C8−GeSe (Figure 3), C9−GeSe (Figure 5) shows now a *parallel* arrangement of the surfactant chains, as has been observed in the corresponding germanium sulfide phases.[13] Therefore, the borderline for a strictly parallel behavior of surfactant chains with the general formula $C_nH_{2n+1}NMe_3^+$ in selenogermanates seems to be at $n = 9$. In terms of studying possible micelle formation, somewhere between $n = 8$ and 9 the $-CH_2-/-CH_2-$ hydrophobic chain−chain interactions seem to be weakened, possibly destroying surfactant organization. Furthermore, the interactions between the inorganic layers (18.1 Å in C9−GeSe and 16.6 Å in C8−GeSe) might start to play a role in the structure formation, which may lead to the crisscross-like arrangement in C8−GeSe. In addition to the surfactant chain arrangements with respect to each other, the alkyl chain conformation of *each* molecule plays a second important role in stabilizing a certain crystal structure. The crystallization process therefore represents a compromise between the need to fill the space between the inorganic layers

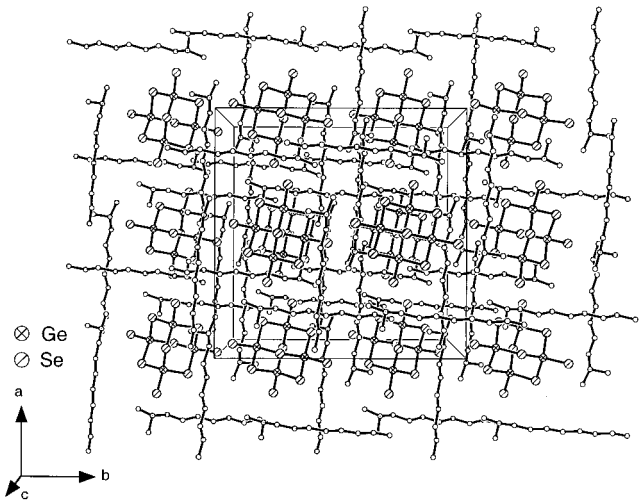

Figure 6. Unit cell of $[n\text{-}C_8H_{17}N(CH_3)_2H]_4Ge_4Se_{10}$ (ODA−GeSe) from the [001] direction. The adamantane clusters are arranged in columns, running down the *c*-axis of the unit cell. The shortest distance between two clusters is 7.27 Å, showing that no interaction takes place. Selected bond lengths (Å): Ge−Se_t, 2.2729(5); Ge−Se_b, 2.3679(5)−2.3779(5); N−C, 1.481(6)−1.490(6); C−C, 1.473(10)−1.526(7).

and the need to satisfy possible alkyl low-energy chain conformations.

ODA−GeSe and Comparison with $[(n\text{-}C_4H_9)_3NH]_4Ge_4Se_{10}$. In contrast to the two compounds discussed above, the structure of $[n\text{-}C_8H_{17}N(CH_3)_2H]_4Ge_4Se_{10}$ (ODA−GeSe) is *nonlamellar*. The lamellar members Cn−GeQ (Se, S) phases of this class of germanium chalcogenides so far prefer triclinic or monoclinic symmetry; ODA−GeSe crystallizes in the higher symmetric *tetragonal* space group $I4_1/a$. The unusual symmetry of this compound is mirrored in its powder diffraction diagram, which clearly reveals that a nonlamellar phase is present (Figure 1D). The structure of ODA−GeSe is rather unusual; instead of displaying adamantane molecule layers, the undistorted $[Ge_4Se_{10}]^{4-}$ clusters are now arranged in a *discrete manner*, each surrounded only by four surfactant molecules within the tetragonal plane (Figures 6 and 7). Although the adamantane units form columns running down the *c*-axis of the unit cell (Figure 6), cluster−cluster distances in this direction can be neglected (Se_t-Se_t > 7.27 Å), since large surfactant chains interacting with neighboring adamantane molecules occupy the space (Figure 6).

The alkyl chain conformation of the only surfactant molecule is strictly all-trans, with torsion angles ranging from 177.30(39)° to 179.71(41)°. As a very interesting feature within the organic−inorganic interface, the nitrogen-bonded hydrogen atom H1 establishes a very close contact to the terminal Se cluster atoms (Figures 6 and 7). At 2.38(5) Å, this N−H···Se hydrogen bridging bond is unusually short (dotted bonds in Figure 7), compared to the theoretical value of 3.0−3.1 Å for the sum of the van der Waals radii of H and Se.[25] It is also shorter than observed values in other compounds showing H···Se hydrogen bridges, e.g. 2.47−2.84 Å in $Na_3AsSe_4{\cdot}9H_2O$ or $Na_3AsO_3Se{\cdot}12H_2O$.[26] Because of these strong Se···H contacts, the compound may alternatively be described as built-up of surfactant cation/Ge_4Se_{10} anion pairs forming *neutral molecular* hybrid cluster units "$[(n\text{-}C_8H_{17})N(CH_3)_2H]_4Ge_4Se_{10}$"; see Figure 7.

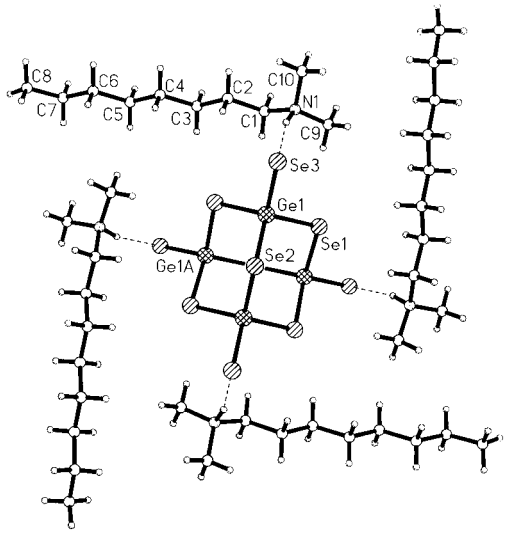

Figure 7. A molecular hybrid single unit "$[n\text{-}C_8H_{17}N(CH_3)_2H]_4Ge_4Se_{10}$" in ODA−GeSe. The strong N−H···Se hydrogen bridge has a length of 2.38(5) Å.

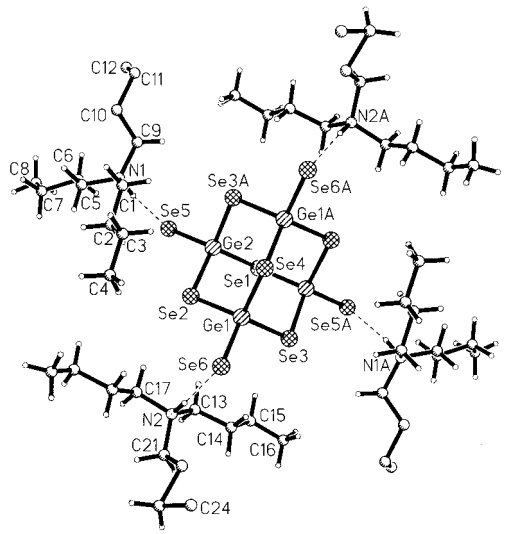

Figure 8. The central molecular unit of $[n\text{-}Bu_3NH]_4Ge_4Se_{10}$. The unit is very similar to the molecular hybrid "$[n\text{-}C_8H_{17}N(CH_3)_2H]_4Ge_4Se_{10}$" in ODA−GeSe (Figure 7). Bond lengths (Å): Ge−Se_t, 2.2645(11)−2.2665(12); Ge−Se_b, 2.3549(11)−2.3741(12); N−C, 1.496(10)−1.537(11); C−C, 1.421(15)−1.61-(3).

Through weak surfactant chain−chain van der Waals interactions these units are assembled in the solid state (Figures 6).

During our efforts to crystallize surfactant-containing selenogermanates with more bulky ammonium headgroups $[(n\text{-}C_4H_9)_3NC_{16}H_{33}]^+$, we inadvertently found a compound containing $[Ge_4Se_{10}]^{4-}$ units charge-balanced by "nonsurfactant cations" $[(n\text{-}C_4H_9)_3NH]^+$ which are a decomposition product of the provided cations. The direct way to synthesize $[(n\text{-}C_4H_9)_3NH]_4Ge_4Se_{10}$ was found to be the stoichiometric reaction of tri-*n*-butylamine with $K_4Ge_4Se_{10}$ under addition of the required amount of protons.

The central structural element of $[(n\text{-}C_4H_9)_3NH]_4Ge_4Se_{10}$ is displayed in Figure 8; it is immediately apparent that both $[(n\text{-}C_4H_9)_3NH]_4Ge_4Se_{10}$ and ODA−GeSe (Figure 7) have substantial similarities in both building units and arrangement. Again each cluster is sur-

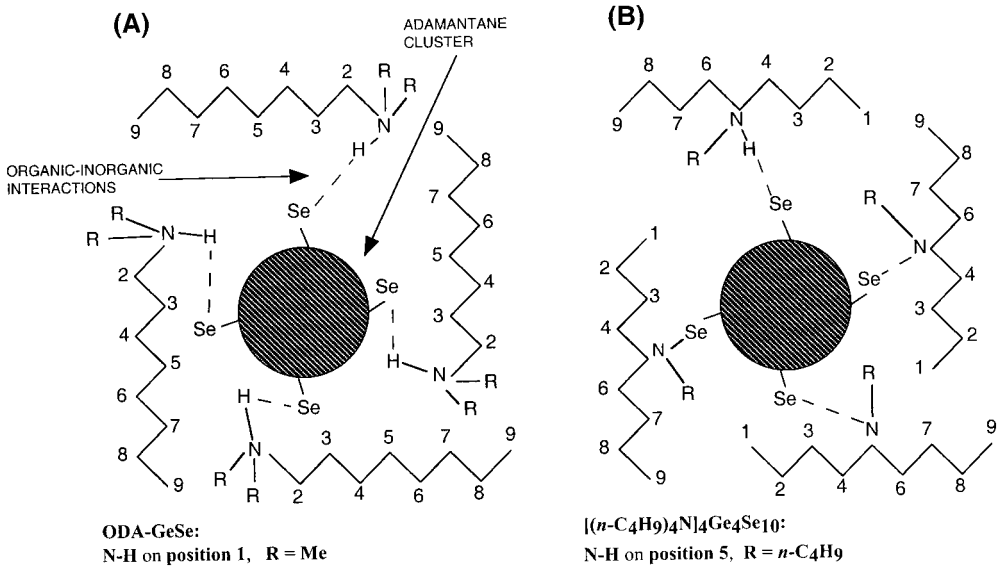

Figure 9. Schematic representation of the similarities between the structures of (A) ODA−GeSe and (B) $[n\text{-}Bu_3NH]_4Ge_4Se_{10}$. Both structures can be described as isolated adamantane clusters that are surrounded by four "C_8N" chains; they differ only in the position of the N−H group and its substituents R (see text for description).

rounded by four *n*-butylammonium cations, whereby each N-bonded hydrogen atom bridges to one of the Se_t atoms of the cluster, leading to a molecular-hybrid unit. We can rationalize both structures if we only consider the chain lengths of the ammonium cations $[(C_8H_{17})NH(CH_3)_2]^+$ and $[(C_4H_9)_3NH]^+$; we can simply describe the structures of ODA−GeSe and $[(n\text{-}C_4H_9)_3NH]_4Ge_4Se_{10}$ as $[Ge_4Se_{10}]^{4-}$ clusters which are each surrounded by four nine-atom chains; see Figure 9. In both compounds these chains are running almost parallel along the adamantane cluster side (Figure 9) and are therefore responsible for isolating the clusters from each other. The differences lie only in the *position* of the N−H group in the "C_8N_1" chain (position 1 in panel A ODA−GeSe; middle position 5 in panel B) $[(n\text{-}C_4H_9)_3NH]_4Ge_4Se_{10}$) as well as the *additional substitution groups* at the N atom (i.e., two methyl groups in ODA−GeSe; one *n*-butyl group in $[(n\text{-}C_4H_9)_3NH]_4Ge_4Se_{10}$). The two N−H···Se hydrogen bridges of $[(n\text{-}C_4H_9)_3NH]_4Ge_4Se_{10}$ are slightly longer (2.406, 2.441 Å) than the ones found in ODA−GeSe but still at the short end of the expected values for this interaction.[26] The single units "$[(n\text{-}C_4H_9)_3NH]_4Ge_4Se_{10}$" are also arranged in columns running down the *b*-axis of the monoclinic unit cell (Figure 10). Each column has four closest neighbors, but compared with ODA−GeSe (see Figure 6), the columns are slightly shifted in their position, giving rise to the lower symmetry monoclinic unit cell (see Figure 10; $\beta = 129.5°$). The alkyl chains of the ammonium cations extend out from the $[Ge_4Se_{10}]^{4-}$ cluster and meet other such chains from neighboring clusters forming van der Waals interactions.

Properties. Raman and far-IR spectra of all compounds proved the presence of undistorted $[Ge_4Se_{10}]^{4-}$ clusters. Panels A and B of Figure 11 show the Raman spectra of C8−GeSe and ODA−GeSe in the region 80−500 cm^{-1}, respectively. The band pattern is very similar to the ones observed in $[Ge_4S_{10}]^{4-}$ [13] or $[Sn_4Se_{10}]^{4-}$ anions,[27] and the assignment can be performed according to their references. The fundamental modes of the adamantane $[Ge_4Se_{10}]^{4-}$ anion with ideal T_d symmetry

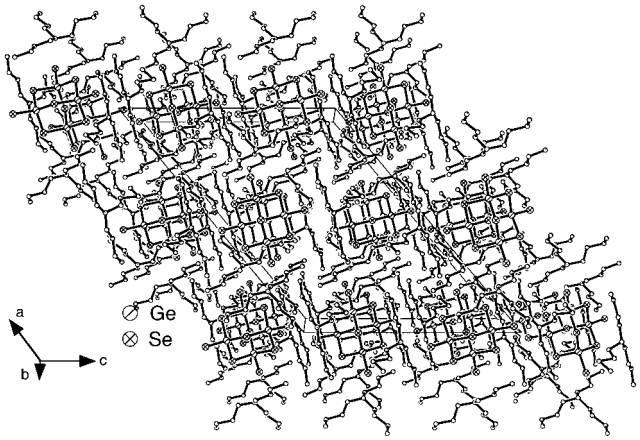

Figure 10. Unit cell of $[n\text{-}Bu_3NH]_4Ge_4Se_{10}$ viewed from the [010] direction.

belong to the irreducible representations $\Gamma = 3A_1 + 3E + 3T_1 + 6T_2$. Hereby, only the A_1, E, and T_2 fundamentals should be Raman active, which means that 12 bands should theoretically be observable. The three A_1 modes can be expected to be strong, since their activity causes large changes in polarizability within the cluster. Whereas ν_2 and ν_3 are caused by modes within the inner Ge_4Se_6 cage, the ν_1 mode is caused by the totally symmetric stretching mode associated with the terminal Ge−Se_t bonds. We assigned these peaks at $\nu_1 = 331$ cm^{-1}, $\nu_2 = 202$ cm^{-1}, and $\nu_3 = 137$ cm^{-1} for C8−GeSe and $\nu_1 = 325$ cm^{-1}, $\nu_2 = 205$ cm^{-1}, and $\nu_3 = 134$ cm^{-1} for ODA−GeSe, respectively. The strong hydrogen bonding in ODA−GeSe is responsible for the weakening of the corresponding Ge−Se_t bond and results in a shift of the associated Raman peaks. The two highest energy modes at 320 and 331 cm^{-1} in C8−GeSe are therefore shifted to 308 and 325 cm^{-1} in ODA−GeSe.

The solid-state UV−vis diffuse reflectance spectra of all phases reported here show that they are insulators

(27) Campbell, J.; DiCiommo, D. P.; Mercier, H. P. A.; Pirani, A. M.; Schrobilgen, G. J.; Willuhn, M. *Inorg. Chem.* **1995**, *34*, 6265.

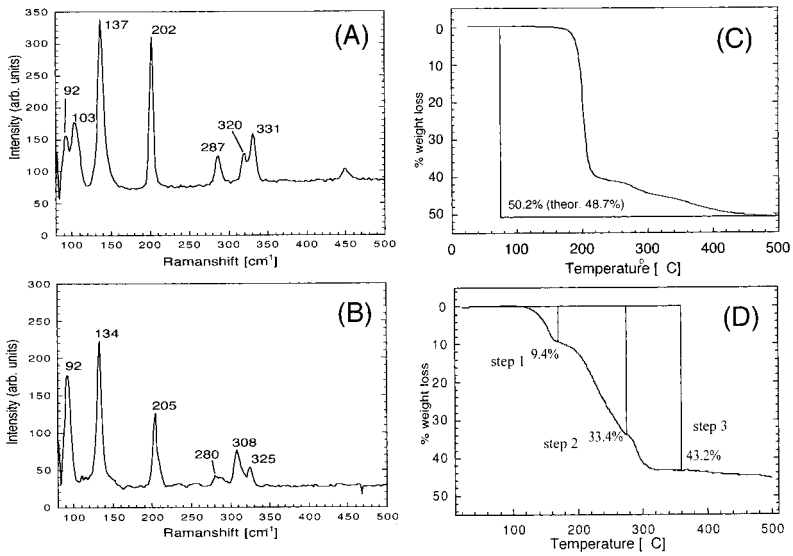

Figure 11. Raman spectra of (A) C8−GeSe and (B) ODA−GeSe. TGA diagrams of (C) C14−GeSe and (D) ODA−GeSe.

or wide band gap semiconductors with values of ∼2.3−2.7 eV at room temperature. The values for C8−GeSe and C9−GeSe are 2.44 and 2.49 eV, respectively. The value for ODA−GeSe is slightly lower, 2.14 eV. The values for the selenides are generally ∼0.5−1 eV lower than those observed for similar sulfide phases, e.g., 3.6 eV for C16−GeS.[13] Such electronic transitions are due to local, molecular excitations involving charge transfer from Se to Ge orbitals.

Thermogravimetric analyses (TGA) of the lamellar C*n*−GeSe phases show that they completely loose the surfactant molecules in a one-step process; see, for example Figure 11C for C14−GeSe. Such a behavior was observed for the corresponding sulfides[13] and persists for other members of the C*n*−GeSe family as well. The residue in all cases is $GeSe_2$, based on X-ray powder diffraction, and its mass is in good agreement with the theoretically calculated one for each C*n*−GeSe compound. A different behavior was observed for the nonlamellar ODA−GeSe. Figure 11D shows that it loses weight between 120 and 320 °C in a three-step process. The first one at ∼120 °C involves a weight loss of 9.1%, which corresponds to the mass of one surfactant equivalent. The second step beginning at 160 °C corresponds roughly to the loss of all four surfactant molecules as volatile amines. The last step between 280 and 320 °C (∼9.3%) could be due to further loss of H_2Se from the compound. An explanation for the first step accompanied by the loss of only one surfactant may be found in a possible rearrangement of the structure and the formation of the compound "[*n*-$C_8H_{17}NMe_2H]_3Ge_4Se_9$-(SeH)". In such a case it is supposed that the surfactant leaves the structure as a neutral amine molecule.

DSC experiments confirm that all C*n*−GeSe phases undergo a solid-state phase transition before melting (and decomposition), as was found earlier in the corresponding Cn−GeS phases.[13] Exemplary values for the transition/melting points are 118.3 °C/211.4 °C for ODA−GeSe and 144.4 °C/193.5 °C C8−GeSe. Similar to our Cn−GeQ phases (Q = S, Se), the CnBr surfactants as well as other compound classes, such as various alkylammonium tetrahalometalates of the general formula $[C_nH_{2n+1}NH_3]_2MX_4$ (M = Co^{2+}, Mn^{2+}, etc.; X = Cl^-, Br^-),[28] also show such transitions before reaching the melting point. These transitions have their origin in changes of the conformation and arrangement of the alkyl chains between the inorganic component layers.

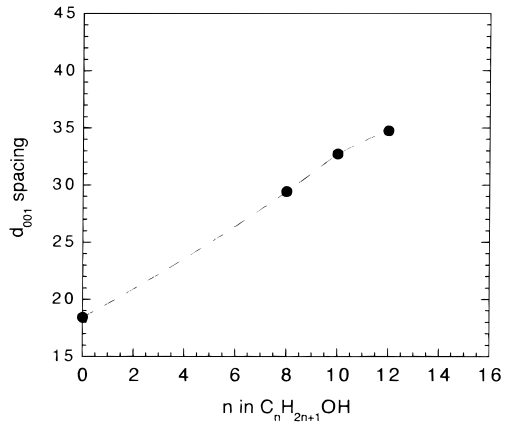

Figure 12. Interlayer spacing of C10−GeSe vs chain length of the absorbed linear alcohol $C_nH_{2n+1}OH$; the expansion from the original spacing of 18.44 Å is 11.01, 13.28, and 16.34 Å for *n*-octanol, *n*-decanol, and *n*-dodecanol, respectively.

Alcohol Absorption. The absorption properties of selected C*n*−GeSe phases as well as ODA−GeSe were examined. All C*n*−GeSe phases readily absorb linear alcohols of various chain length, from MeOH to *n*-dodecanol. The absorption is in all cases accompanied by an almost linear expansion of the interlayer distance, as indicated by the shift of the low-angle Bragg peaks. This is in accordance with the corresponding sulfur phases Cn−GeS.[13] Figure 12 exemplifies this behavior on C10−GeSe; its original interlayer distance of 18.44 Å is expanded to 29.45, 32.72, and 34.78 Å upon absorption of *n*-octanol, *n*-decanol, and *n*-dodecanol, respectively. These intercalated products are usually stable for weeks. Since the process is reversible, subsequent desorption shifts the peaks back to their original position. Whereas desorption occurs fast at room temperature for short alcohols (MeOH, EtOH), the

(28) (a) Cajolo, M. R.; Corradini, P.; Pavone, V. *Acta Crystallogr.* **1977**, *B33*, 553. (b) Guo, N.; Lin, Y.-H.; Xi, S.-Q. *Acta Crystallogr.* **1995**, *C51*, 617.

compounds have to be heated slightly for higher alcohols to accelerate it.

Alcohol absorption was also investigated for the nonlamellar ODA−GeSe. In contrast to the C*n*−GeSe phases described above, we could not observe any changes in the powder pattern, even after prolonged exposure. This important observation allows us to speculate about the mechanism of such an absorption process. ODA−GeSe possesses strong N−H····Se bridges at the organic−inorganic interface, which obviously hinders the compound from absorbing alcohols. On the other hand, the lamellar C*n*−GeSe phases lacking this kind of interaction can absorb appropriate molecules fast and reversibly. This suggests that the absorbed molecules may occupy the space where these interactions take place, i.e., *between the organic/inorganic interface* and not, for example, in the space between the surfactant alkyl chains. The strong N−H····Se bridges, expressed through very short H···Se distances, prevent such an "insertion" in ODA−GeSe. Another possibility for the absorption process in C*n*−GeSe which cannot be completely ruled out would be the removal of the surfactant chain interdigitation with simultaneous insertion of the alcohol between the alkyl chain tails, although absorption experiments on $[C_nH_{2n+1}NH_3]_4Ge_4S_{10}$ compounds support the former mechanism.[29]

Concluding Remarks

Our investigations of surfactant containing selenogermanate adamantane $[Ge_4Se_{10}]^{4-}$ phases led to a number of new lamellar compounds C*n*−GeSe with $n = 8, 9, 10, 12, 14, 16, 18$. The structural characterization of the first two members of this family, C8−GeSe and C9−GeSe, provides new insights into the behavior of the surfactant chain conformation and arrangement at the "shorter end" of alkyltrimethylammonium molecule series, i.e., the transition from "surfactant-" to "nonsurfactant-like" countercations. Whereas C9−GeSe (and higher C*n*−GeSe) shows strictly parallel alkyl chains, with half of the chains extended and the other half bent approximately in the middle of the chain,[13] the surfactants in C8−GeSe behave differently and show a crisscross-like arrangement. C8−GeSe and C9−GeSe and all higher lamellar C*n*−GeSe phases show only weak C−H···Se van der Waals interactions at their organic−inorganic interface.

If one of the methyl groups in C8−GeSe is formally exchanged with a hydrogen atom, it generates a surfactant with a source of acidic protons, potentially giving rise to strong N−H···Se bridges. The latter are indeed observed in $[n\text{-}C_8H_{17}N(CH_3)_2H]_4Ge_4Se_{10}$ (ODA−GeSe),-which somewhat surprisingly is a nonlamellar phase. C8−GeSe and ODA−GeSe are vivid examples for the enormous impact of apparently slightly changed conditions on structural outcome. Unlike C8−GeSe, ODA−GeSe reveals strong N−H····Se hydrogen bonds, which lead to an entirely new structure type concerning the surfactant/adamantane arrangement to *isolated* "$[n\text{-}C_8H_{17}N(CH_3)_2H]_4Ge_4Se_{10}$" units. Furthermore, unlike all lamellar C*n*−GeSe phases, the strong N−H····Se bridges in ODA−GeSe might now be responsible for the fact that ODA−GeSe does *not* absorb primary alcohols, giving some insight into the mechanism of such a process for lamellar, surfactant-containing phases. Such lamellar C*n*−GeSe phases may potentially be used in certain cases to remove alcohols from water.

Acknowledgment. Support from the National Science Foundation CHE 99-03706 (Chemistry Research Group) is gratefully acknowledged. Part of this work was carried out using the facilities of the Center for Electron Optics of Michigan State University. M.W. thanks the Deutsche Forschungsgemeinschaft for a postdoctoral research fellowship.

Supporting Information Available: Tables of positional and thermal anisotropic thermal parameters of all atoms, bond distances and angles for ODA−GeSe, C8−GeSe, C9−GeSe and $[n\text{-}Bu_3NH]_4Ge_4Se_{10}$. This material is available free of charge via the Internet at http://pubs.acs.org.

CM000102O

(29) Rangan, K. K.; Kanatzidis, M. G. Manuscript in preparation.